Available online at www.sciencedirect.com

ScienceDirect

Procedia CIRP 62 (2017) 458 – 463

www.elsevier.com/locate/procedia

10th CIRP Conference on Intelligent Computation in Manufacturing Engineering - CIRP ICME '16

Experimental analysis of residual stresses on AlSi10Mg parts produced by means of Selective Laser Melting (SLM)

Alessandro Salmi*, Eleonora Atzeni, Luca Iuliano, Manuela Galati

Politecnico di Torino, Department of Management and Production Engineering, C.so Duca degli Abruzzi, 24, 10129 Torino, Italy

* Corresponding author. Tel.: +39-011-090-7210; fax: +39-011-090-7299. *E-mail address:* alessandro.salmi@polito.it

Abstract

During the Selective Laser Melting (SLM) process, the scanned layers are subjected to rapid thermal cycles. Steep temperature gradients generate residual stresses. Residual stresses can be detrimental to the proper functioning and the structural integrity of built parts. In this paper, the semi-destructive hole-drilling method has been used to measure the residual stresses on AISi10Mg parts after building, stress relieving and shot-peening, respectively. The outcomes have shown the presence, on the as-built components, of high tensile stresses that the usual post-processing operations are not able to minimize. The adopted method has proved to be a suitable tool to identify optimal process parameters for each step of the production cycle.

Peer-review under responsibility of the scientific committee of the 10th CIRP Conference on Intelligent Computation in Manufacturing Engineering

Keywords: Residual stresses; Selective Laser Melting; AlSi10Mg; Hole-drilling method; Stress relieving; Shot-peening

1. Introduction

The selective laser melting process (SLM) utilizes a laser-beam to melt metal powder and produce components of elevated geometrical complexity. The powder absorbs a fraction of the laser's energy flow. This is converted into heat through electronic interactions with the atoms on the surface of the powder, which in turn causes the fusion of the powder and elevated thermal gradients. Production processes that utilize a laser as an energy source, such as soldering and laser bending, are known to induce large quantities of residual stresses because of the high temperature gradients that are generated on the components [1, 2]. In the case of the SLM process, the residual stresses can cause distortions, cracks and delamination between the subsequent layers of the components [3-6]. There are a great many similarities between the residual stresses that develop during a multi-pass welding process and those that develop during the SLM process; both processes in fact lead to the heating of the material that is deposited layer-by-layer. Although the welding process has been studied in great detail, the same cannot be said about the study of the stresses that develop during the SLM process of metal powder. In fact, very few experimental or numerical research papers are available in the literature concerning the study of residual stresses associated with the components produced by means of the SLM process.

The residual stresses created during the SLM process are the sum of the effects of hardening derived from the rapid solidification of the sections and of the volumetric changes caused by both the temperature gradients and by the phase transformations, including the solidification and the phase changes to a solid state between crystalline structures [7]. The differences in temperature in the irradiated region produce transient thermal deformations on the surface and at a depth. When the source of heat is removed, the material cools down and contracts more than the material that is present in the surrounding zone and residual stresses are thus created. The work by Mercelis and Kruth [7] supplies descriptions of the development of the residual stresses that seem to be generated by a similar process to that of the Temperature Gradient Mechanism (TGM), in which the thermal expansion and contraction of the material during the heating and cooling phases that follow the laser interaction induce step-like temperature gradients in all of the irradiated region. The heated

Peer-review under responsibility of the scientific committee of the 10th CIRP Conference on Intelligent Computation in Manufacturing Engineering
doi:10.1016/j.procir.2016.06.030

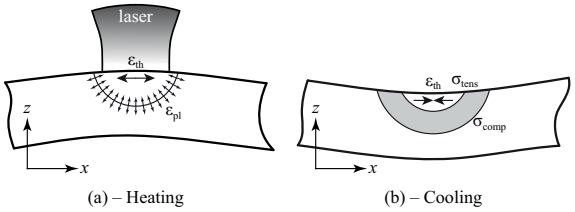

Fig. 1. Temperature gradient mechanism (TGM) in laser-based additive manufacturing systems [8].

material and the solid surrounding material can be assimilated to a structural unbalance that effectively restrains the movement of the heated metallic material when the latter changes in state. During the cooling, a complex contraction of the irradiated region takes place, that is a tension state, while the material that surrounds the irradiated zone undergoes an expansion that results in a compression state. The volumetric shrinking of the material melted during the cooling induces compression stresses in the surrounding material, which is under the influence of the temperature gradient, as illustrated in Figure 1 [8]. Gusarov, Pavlov and Smurov [9] proposed a thermos-elastic model, which showed that longitudinal tensile stresses are on average two times greater than transversal ones. The model explains the formation of two longitudinal and transversal crack systems that were observed during experiments. The *island scanning* strategy of some SLM machines can reduce residual stresses by shortening the scan tracks [10]; the rotation of the scan pattern between layers is another adopted solution that is able to create a more uniform stress distribution by compensating for directional anisotropy.

Some studies can be found in the literature that have had the aim of evaluating the distribution of the stresses in the different longitudinal, transversal and normal directions, with reference to parallelepiped samples of thin walls in order to simplify the analysis. The results show that the stresses in the longitudinal direction are greater and that they reduce as they come closer to the base of the component. Compression states are generally observed in the center of the samples, which then become traction states as they approach the surface [11-13]. Other studies on residual stresses are of a qualitative or semi-quantitative type and are based on the evaluation of the deformations of bridge or cantilever structures [10]. Furthermore, the forecasting of the residual stresses and distortions induced during laser melting have proved to be a hard task because of the high localized temperatures, of the rapid temperature cycles and of the source of heat in movement, due to the use of a laser.

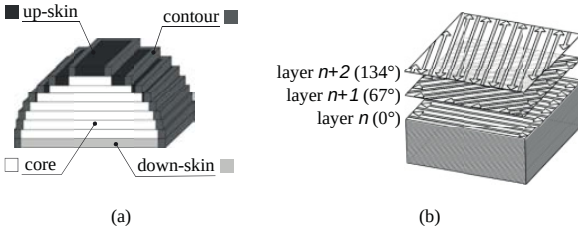

Fig. 2. (a) Schematization of the structure of the downskin, upskin and core parts; (b) exposition of each layer to the laser [14].

This work describes an experimental activity that has made it possible to draw the trend of the residual stresses on the upper layers of samples produced in AlSi10Mg aluminum alloy by means of an SLM process in order to evaluate how such stresses are altered by the different phases of the production process, starting from the production to the thermal treatment and going on to removal of the supports and the final shot-peening treatment.

2. Materials and Methods

Eight parallelepiped 30 × 20 × 10 mm³ samples in EOS AlSi10Mg aluminum alloy were produced in a single job using an SLM EOSINT M 270 eXtended machine. The layer was 30 µm thick and the building platform was kept at 35° C. The components were constructed while blowing argon into the work chamber in order to avoid oxidation of the material. A standard construction strategy, which foresees different exposition parameters for the core, the skin, and the contour was adopted. The first two layers of the base of the components have been termed *downskin*, while the last three at the top have been termed *upskin*. The layers compressed between the downskin and the upskin represent the *core*. A schematization of the structure is shown in Figure 2a with the downskin, upskin and core parts. After the contouring phase of the core region has been completed, the contour of each layer is exposed to a low power laser in order to improve the surface finishing of the part [14]. The pattern of the exposition to the laser beam is shown in Figure 2b. The scan lines of each layer within the core area have been rotated by 67° to the scan line of the preceding layer. Table 1 reports the values of the parameters utilized during the construction of the components [14].

Immediately after the construction, the table (Figure 3a) was removed from the machine and the residual stresses on the first two samples, indicated with the letters A and B, were evaluated. Sample A was prepared without supports, while sample B was prepared with supports. After the measurement, the platform with the samples was subjected to a stress relieving thermal treatment at 300° C for 3 hours. Other evaluations of the residual stresses were conducted on samples C and D, without and with supports, respectively, in order to evaluate the release of the stresses generated by the thermal treatment. Subsequently, samples E and F were removed from the platform and the shot-peening process of the surface was conducted. A NORBLAST SD9 shot-peening machine was used for the shot-peening treatment, utilizing 200 µm diameter zirconia beads and a pressure of 3 bar. A 6 mm nozzle was kept inclined at 45° to the treated surface. After the finishing operation, the samples were again measured in order to evaluate the final residual stress state.

Table 1. Process parameters utilized for the production of the samples [14].

Parameters	Skin	Core	Contour
Scan speed [mm/s]	900	800	900
Laser power [W]	120	195	80
Hatch distance [mm]	0.10	0.17	–
Layer thickness [µm]	30		
Laser spot diameter [µm]	10		

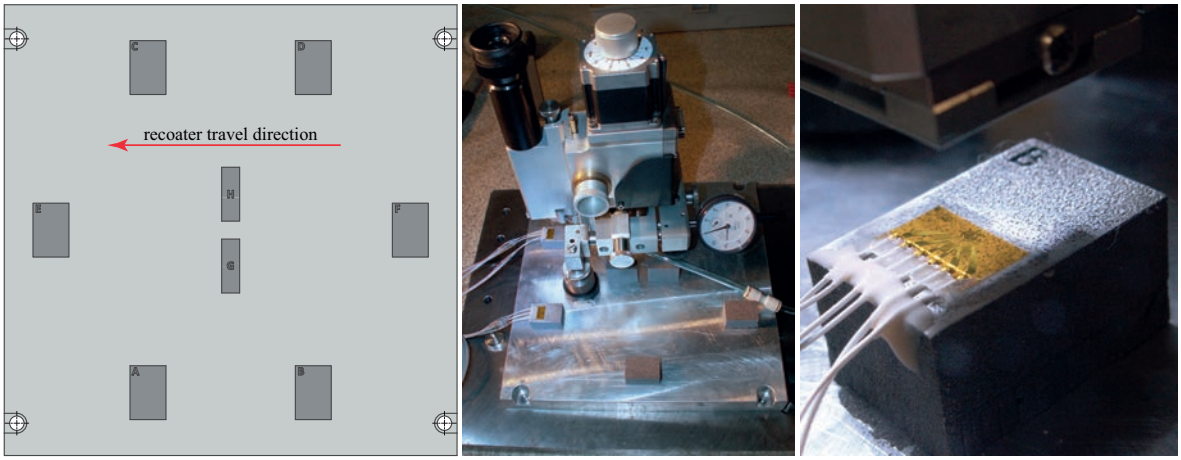

(a) (b) (c)

Fig. 3. (a) Schematic illustration of the platform with the eight samples; (b) MTS3000 RESTAN (REsidual STress ANalyzer) system by SINT Technology positioned on the construction platform with the samples; (c) Glued rosette strain gauge and cable blocking.

2.1. Evaluation of the residual stresses according to the ASTM E837-13a standard

An MTS3000 RESTAN (Figure 3b) system by SINT Technology, which is based on the hole drilling strain gauge method, was used to measure the residual stresses [15]. The measurement of the residual stresses by means of the hole drilling strain gauge method involves drilling a small hole in the center of a three grid strain gauge rosette. The strains released by the tested material are acquired for each drilling step and are used to calculate the residual stresses according to the ASTM E837-13a standard [15]. A 2 mm diameter drill bit is used to produce a 1.2 mm deep flat-bottom hole, with a sequence of 24 drilling steps of 50 µm. A K-RY61-1.5/120R rosette strain gauge made by HBM was utilized during the experimental campaign. An image of the rosette strain gauge installed on sample B is shown in Figure 3c.

The program for the calculation of the residual stresses from the measurement data was developed entirely in MATLAB R2009a and the trend of the residual stresses in the thickness of the sample was evaluated with the Integral Method, as suggested in the ASTM E837-13a standard [15]. Because of the type of mathematical relation that exists between the released deformations and the residual stresses and due to the fact that it is not possible to carry out direct calibration procedures, the elaborated evaluation method has resulted to be very sensitive to measurement errors. In fact, the mathematical relations that exist between the released deformations and the residual stresses are badly conditioned. Therefore, a remarkable amount of noise can easily occur under the form of local oscillations in the calculated stresses. However, the application of smoothing techniques can lead to improvements in both the accuracy and in the resolution. For this reason, even though the ASTM E837-13a standard does not foresee it, the numerical values of the released deformations acquired during the experimental campaign were filtered by means of a polynomial interpolation, in which the degree of the polynomial was chosen so as to approximate the experimental data as much as possible and to eliminate fluctuations due to random errors. Eighth grade polynomials were used in the conducted analyses as it has been observed that in problems characterized by a great number of data, as in the here analyzed case, increasing the degree of the polynomial does not always lead to a better interpolation of the data. In fact, polynomials of an elevated degree can show an oscillating trend among the experimental points [16].

3. Results and Discussion

The results of the numerical elaborations conducted according to the previously described procedure are presented hereafter. Moreover, the evolution of the profile of the residual stresses of the samples is illustrated in function of the process phase (as-built, after the thermal treatment, after shot-peening) for samples with and without supports.

3.1. Trend of the residual stresses for as-built samples with and without supports

The trends of the main residual stresses are shown in Figure 4 in function of the depth. It can be observed that there are residual traction stresses in the thickness analyzed for both samples. However, sample B constructed with the supports shows a greater stress state than that in sample A, which was constructed directly in contact with the support plate. This different behavior of the samples, according to the construction characteristics, could be due to the different heat transmission modalities along the building direction: sample A in fact has an exchange surface toward the platform that is equal to its section, while the exchange section for sample B is limited to the support section, as the unsintered powder has a thermal exchange coefficient that is at least one order of magnitude lower [17]. This means that the thermal gradient is lower for sample A and, as a consequence, so is the residual stress state in the component. Moreover, as far as the residual stresses in sample B are concerned, it can be observed that the stress reaches a value of about 320 MPa at a depth of 0.8 mm, and the

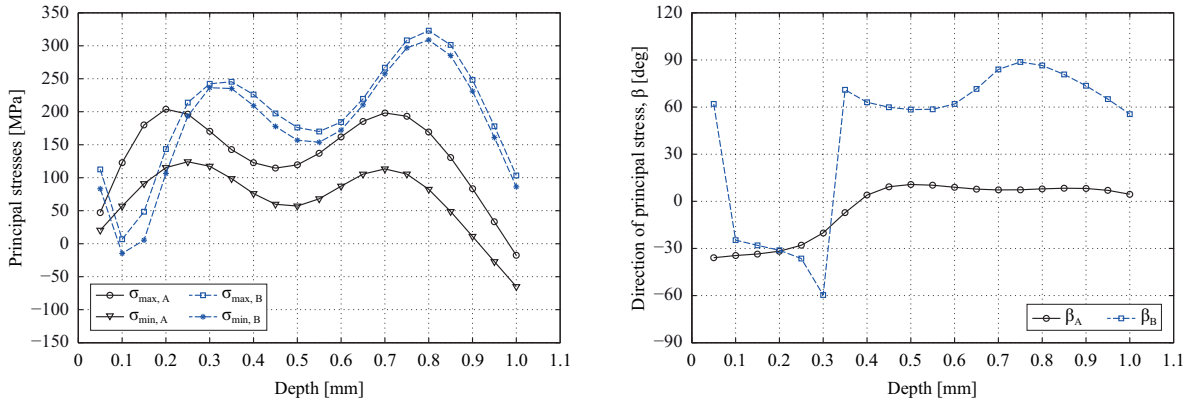

Fig. 4. Comparison of the as-built samples constructed without and with supports.

residual stresses therefore surpass the yielding strength of the material. Moreover, the trend of the residual stresses shown in Figure 4 is oscillating. This could be due to the fact that the residual stresses generated during the SLM process are the sum of the stresses due to hardening phenomena derived from the solidification of the deposited layers and of the thermal stresses due to the lack of correspondence between the thermal expansion and the stiffness of the different layers of the material during the process. The oscillating trend of the stresses is similar to the trend of the residual stresses that develop during a multi-pass welding process [18, 19]. As far as angle β, which describes the main direction of the stresses in function of the depth (Figure 4), is concerned, abrupt variations in the values can be observed. The authors first hypothesized that the variations could be connected to the construction strategy adopted for the components, which foresees the rotation of the scanlines by 67° to the previous layer.

3.2. Trend of the residual stresses for samples after the thermal treatment with and without supports

A comparison of the trends of the main residual stresses in function of the depth is shown in Figure 5 for the two samples constructed without supports: sample A (as-built) and sample C after the stress relieve thermal treatment. It can be observed that both of the trends have an oscillating nature, and that the maximum and minimum points are at about the same depth. Moreover, it is also possible to note that both of the samples are characterized by a tension state of stress, even though a notable reduction in the stress state can be seen for sample C. In fact, the stress state on average was observed to have reduced by about 100 ÷ 150 MPa after the thermal treatment. A variation of the β angle can be observed, although its oscillatory behavior persists.

The main residual stresses and the β angle of orientation of the two samples constructed with the supports, that is, sample B (as-built) and sample D after the stress release thermal treatment, are compared in Figure 6. By analyzing Figure 6, it can be seen that the thermal treatment results in greater benefits: the traction stress state is reduced by about 200 MPa and it settles at around 50 MPa, with contained oscillations. The greater stress relieve can be explained by considering the supports as a non-perfectly rigid constraint between the plate and the component, so that stresses are released and, as a consequence, the sample is deformed. Again in this case, it can be observed that the stress state takes on relative maximum and minimum values at about the same depth of the untreated sample. Finally, by examining the trends in the main direction, which are shown in Figure 6, the oscillatory trend of the values assumed by the β angle can be confirmed. The thermal

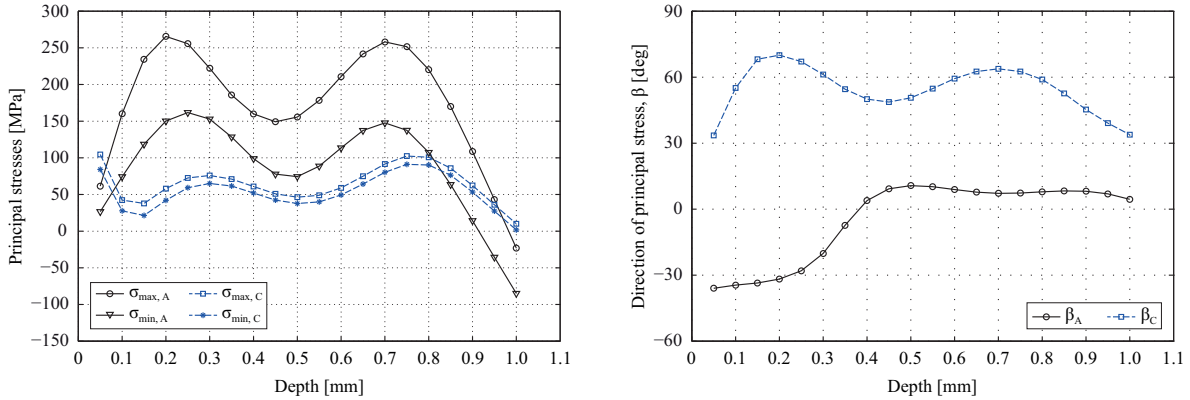

Fig. 5. Comparison of the samples constructed without supports before and after undergoing the stress release thermal treatment.

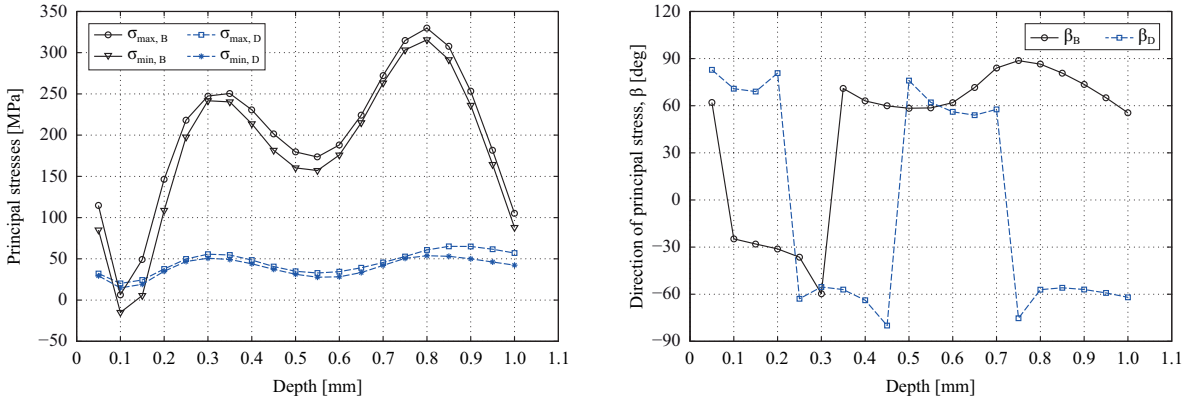

Fig. 6. Comparison of the samples constructed with supports before and after undergoing the stress release thermal treatment.

treatment has accentuated the oscillations with an inversion in direction at about each 0.2 mm of depth.

3.3. Trend of the residual stresses for samples after the thermal treatment following the shot-peening with supports

The residual stresses and their angle of orientation in the two samples constructed with supports, that is, sample B (as-built), sample D (post thermal treatment) and sample F after the shot-peening treatment, are compared in Figure 7. The effectiveness of the shot-peening treatment can be observed from an analysis of Figure 7. A superficial compression state is in fact generated (for a depth of about 0.05 ÷ 0.10 mm), with a further general reduction in the tension stress state along the depth. It can be confirmed that the trend of the stress state in the various samples takes on relative maximum and minimum values at about the same depth. A further reduction in the spread of the oscillations of the residual stress can be observed following the shot-peening treatment. The oscillatory trend of the values of the β angle can also be observed in Figure 7 for the shot-peened sample. It can be noted that the oscillations almost overlap those of sample D, but there is a translation at a depth. It can be hypothesized that such behavior is the consequence of the zero-setting adopted during the various measurements.

4. Conclusions

In the present work, the residual stress state of samples in an AISi10Mg alloy produced by means of SLM technology has been evaluated. The experimental campaign has made it possible to evaluate the trend of the residual stresses to a depth of 1 mm, in function of the process phase and the presence or lack of supports. The results have pointed out that:

- direct contact between the sample under construction and the support plate (in other words, with or without supports) has a significant effect on the entity and trend of the residual stress state;
- the values of the residual stresses have an oscillatory nature and these oscillations are maintained (although with an ever decreasing spread) even after thermal and shot-peening treatments;
- the adopted stress relief thermal treatment (standard thermal treatment suggested by the producer) has not been sufficient to release all the stresses and the sample has remained, at least for the analyzed depth, in a state of tension;
- the shot-peening treatment has allowed not only a superficial compression state to be created but has also allowed the overall stress state, relative to the analyzed depth, to be made uniform.

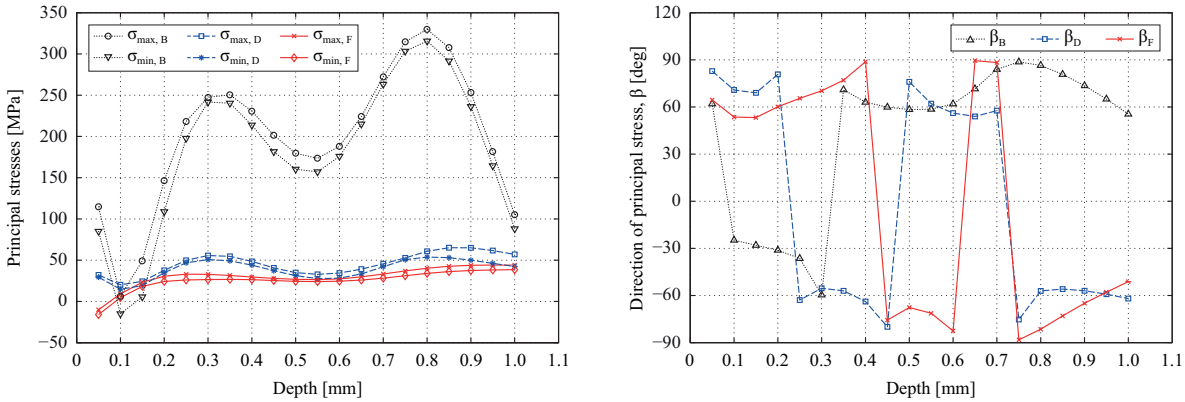

Fig. 7. Comparison of the samples constructed with supports in the as-built, post thermal treatment and post shot-peening condition.

Possible future developments could involve the metallographic analyses of samples in order to correlate the residual stress state to the microstructure of the component and/or the construction process of the layers, the evaluation of the residual stresses after machining operations and the optimization of the stress relief thermal treatments in order to reduce the residual traction stress state to a minimum and to make the shot-peening operation more effective for the creation of a residual stress profile in compression below the surface.

Acknowledgements

The authors would like to acknowledge the assistance of Dr. Sergio Aulico in facilitating the MATLAB programming and the support of Mr. Giovanni Marchiandi during the measurement phase. Moreover, the authors extend their thanks to Dr. Flaviana Calignano and Dr. Francesco Trevisan (Istituto Italiano di Tecnologia, Center for Space Human Robotics IIT@Polito, Torino, Italy) for their help and support in the research.

References

[1] Y. Chen, I.C. Sheng, Residual Stress in Weldment, Journal of Thermal Stresses, 15 (1992) 53-69.
[2] B.S. Yilbas, S.S. Akhtar, Laser bending of metal sheet and thermal stress analysis, Optics & Laser Technology, 61 (2014) 34-44.
[3] K. Kempen, B. Vrancken, S. Buls, L. Thijs, J. Van Humbeeck, J.P. Kruth, Selective Laser Melting of Crack-Free High Density M2 High Speed Steel Parts by Baseplate Preheating, J Manuf Sci E-T Asme, 136 (2014).
[4] M. Alimardani, E. Toyserkani, J.P. Huissoon, C.P. Paul, On the delamination and crack formation in a thin wall fabricated using laser solid freeform fabrication process: An experimental–numerical investigation, Optics and Lasers in Engineering, 47 (2009) 1160-1168.
[5] E.O. Olakanmi, R.F. Cochrane, K.W. Dalgarno, A review on selective laser sintering/melting (SLS/SLM) of aluminium alloy powders: Processing, microstructure, and properties, Prog Mater Sci, 74 (2015) 401-477.
[6] B. Vrancken, V. Cain, R. Knutsen, J. Van Humbeeck, Residual stress via the contour method in compact tension specimens produced via selective laser melting, Scripta Materialia, 87 (2014) 29-32.
[7] P. Mercelis, J.P. Kruth, Residual stresses in selective laser sintering and selective laser melting, Rapid Prototyping J, 12 (2006) 254-265.
[8] J.P. Kruth, X. Wang, T. Laoui, L. Froyen, Lasers and materials in selective laser sintering, Assembly Autom, 23 (2003) 357-371.
[9] A.V. Gusarov, M. Pavlov, I. Smurov, Residual Stresses at Laser Surface Remelting and Additive Manufacturing, Physcs Proc, 12 (2011) 248-254.
[10] J.P. Kruth, J. Deckers, E. Yasa, R. Wauthle, Assessing and comparing influencing factors of residual stresses in selective laser melting using a novel analysis method, P I Mech Eng B-J Eng, 226 (2012) 980-991.
[11] J. Ding, P. Colegrove, J. Mehnen, S. Ganguly, P.M.S. Almeida, F. Wang, S. Williams, Thermo-mechanical analysis of Wire and Arc Additive Layer Manufacturing process on large multi-layer parts, Comp Mater Sci, 50 (2011) 3315-3322.
[12] M.L. Griffith, R.B. Rogge, T.M. Holden, P. Rangaswamy, Residual stresses in components formed by the laserengineered net shaping (LENS) process, The Journal of Strain Analysis for Engineering Design, 38 (2003) 519-527.
[13] P. Rangaswamy, M.L. Griffith, M.B. Prime, T.M. Holden, R.B. Rogge, J.M. Edwards, R.J. Sebring, Residual stresses in LENS (R) components using neutron diffraction and contour method, Mat Sci Eng a-Struct, 399 (2005) 72-83.
[14] D. Manfredi, F. Calignano, M. Krishnan, R. Canali, E. Ambrosio, E. Atzeni, From Powders to Dense Metal Parts: Characterization of a Commercial AlSiMg Alloy Processed through Direct Metal Laser Sintering, Materials, 6 (2013) 856-869.
[15] ASTM E837-13a, Standard Test Method for Determining Residual Stresses by the Hole-Drilling Strain-Gage Method, ASTM International, West Conshohocken, PA, 2013, http://www.astm.org/.
[16] L.M. Kocic, G.V. Milovanovic, Shape preserving approximations by polynomials and splines, Comput Math Appl, 33 (1997) 59-97.
[17] N.E. Hodge, R.M. Ferencz, J.M. Solberg, Implementation of a thermomechanical model for the simulation of selective laser melting, Comput Mech, 54 (2014) 33-51.
[18] T.-L. Teng, P.-H. Chang, W.-C. Tseng, Effect of welding sequences on residual stresses, Computers & Structures, 81 (2003) 273-286.
[19] M. Chiumenti, M. Cervera, A. Salmi, C. Agelet de Saracibar, N. Dialami, K. Matsui, Finite element modeling of multi-pass welding and shaped metal deposition processes, Computer Methods in Applied Mechanics and Engineering, 199 (2010) 2343-2359.